

Radiative decays of the spin-2 partner of $X(3872)$

Pan-Pan Shi,^{1,2,*} Jorgivan M. Dias,^{1,†} and Feng-Kun Guo^{1,2,3,‡}

¹*CAS Key Laboratory of Theoretical Physics, Institute of Theoretical Physics,
Chinese Academy of Sciences, Beijing 100190, China*

²*School of Physical Sciences, University of Chinese Academy of Sciences, Beijing 100049, China*

³*Peng Huanwu Collaborative Center for Research and Education, Beihang University, Beijing 100191, China*

It has been generally expected that the $X(3872)$ has a spin-2 partner, X_2 , with quantum numbers $J^{PC} = 2^{++}$. In the hadronic molecular model, its mass was predicted to be below the $D^*\bar{D}^*$ threshold, and the new structure reported in the $\gamma\psi(2S)$ invariant mass distribution by the Belle Collaboration with mass $M = (4014.3 \pm 4.0 \pm 1.5)$ MeV and decay width $\Gamma = (4 \pm 11 \pm 6)$ MeV, with a global significance of 2.8σ , is a nice candidate for it. We consider the radiative decay widths for the $X_2 \rightarrow \gamma\psi$ with $\psi = J/\psi, \psi(2S)$ treating the X_2 as a $D^*\bar{D}^*$ shallow bound state, and estimate the events of X_2 in two-photon collisions that can be collected in the $\gamma J/\psi \rightarrow \gamma\ell^+\ell^-$ ($\ell = e, \mu$) final states at Belle. Based on the upper limit for the ratio of decay widths of $X(3872) \rightarrow \gamma\psi(2S)$ and $X(3872) \rightarrow \gamma J/\psi$ measured by BESIII, we predict the similar ratio $\Gamma(X_2 \rightarrow \gamma\psi(2S))/\Gamma(X_2 \rightarrow \gamma J/\psi)$ to be smaller than 1.0. We suggest searching for the X_2 signal in the $\gamma J/\psi$ invariant mass distribution via two-photon fusions. The results will lead to insights into both the $X(3872)$ and the new structure observed by Belle.

* shipanpan@itp.ac.cn

† jorgivan.mdias@itp.ac.cn

‡ fkguo@itp.ac.cn

I. INTRODUCTION

The hadron spectroscopy of mesons and baryons with heavy quarks (charm and bottom) has been an important laboratory in the quest for understanding quantum chromodynamics (QCD) at the confinement scale due to the large bulk of experimental information accumulated over the last two decades. Many new hadronic states observed in the heavy sector seem to not fit into the predictions from the potential quark models such as the well-known Godfrey-Isgur quark model [1]. This fact has triggered a debate about the nature of those hadrons, and assumptions of different multiquark configurations beyond the conventional quark-antiquark/three quarks were put forward in order to explain their properties, such as mass, decay width, and the J^{PC} quantum numbers, *i.e.*, the total angular momentum J , parity P , and charge conjugation C (see the reviews [2–13]).

Among these models, the molecular picture seems to be a natural one since the majority of the new hadrons are near some hadron-hadron threshold. In the charm sector, for instance, the $X(3872)$ state is just at the $D\bar{D}^*$ ($\bar{D}D^*$) threshold, and its properties are suitably described considering the $X(3872)$ as a $D\bar{D}^*$ molecular state (for a review focusing on the hadronic molecular model of the $X(3872)$, see Ref. [14]). In fact, the $X(3872)$ was the first among those new hadrons observed experimentally by the Belle Collaboration in 2003 [15], with $J^{PC} = 1^{++}$ quantum numbers determined by the LHCb Collaboration a decade later [16]. It is, to date, the most well-studied state, and it is not a surprise that its experimental and theoretical information is used as inputs for predictions of new hadronic states in the heavy quark sector. In Ref. [17], the authors assumed the $X(3872)$ as a $D\bar{D}^*$ molecule and concluded that a $D^*\bar{D}^*$ state should exist as a consequence of the heavy-quark spin symmetry for the system under consideration. Specifically, using a contact-range (pionless) effective field theory, they claimed that the new state, from now on called X_2 , is the spin-2 partner of the $X(3872)$, with a similar value for the binding energy and mass of about 4012 MeV. Such a state was first predicted in Ref. [18] long ago with a mass $M = 4015$ MeV and later in Refs. [17, 19–34] using various phenomenological models.

Recently, the Belle collaboration reported a hint of an isoscalar structure with mass $M = (4014.3 \pm 4.0 \pm 1.5)$ MeV and width $\Gamma_{X_2} = (4 \pm 11 \pm 6)$ MeV, seen in the $\gamma\psi(2S)$ invariant mass distribution via a two-photon process [35]. The global significance is 2.8σ . This new structure is located near the $D^*\bar{D}^*$ threshold which leads us to conclude that it is a promising candidate for the $D^*\bar{D}^*$ shallow bound state.¹ In addition, the mass value predicted in Refs. [17, 23] is in good agreement with the experimental one reported by Belle [35], and the measured width well matches

¹ In Refs. [36, 37], this structure was assumed to be a $D^*\bar{D}^*$ molecule with $J^{PC} = 0^{++}$.

the predicted one, of the order of a few MeV, in Ref. [27] despite that there is a sizeable uncertainty in the theoretical predictions [27, 28]. Thus, this narrow structure could be a hint for the X_2 state, supporting the theoretical predictions in Refs. [17, 18, 23].

Alternatively, by looking at the spectra of tetraquarks, there also exists spin partners of 1^{++} states that reproduce the 2^{++} quantum numbers of X_2 as well as its mass [38–41]. Although the authors of these works were not particularly aiming at the X_2 state, it is still possible to assign the results to such a structure. On the other hand, a 2^{++} tensor state with a similar mass could also be described as a conventional $2P$ charmonium state [1, 42]; in this case, the $\chi_{c2}(3930)$ [43] would be an exotic meson.

One way to disentangle those different multiquark configurations from the molecular point of view is to check the mass splitting between the 2^{++} and 1^{++} states. In Refs. [17, 23], the corresponding mass splitting is approximately equal to that between the vector and pseudoscalar charmed mesons, that is

$$m_{X_2} - m_X \sim m_{D^*} - m_D \sim 140 \text{ MeV}, \quad (1)$$

with $m_D(m_{D^*})$ the pseudoscalar (vector) charmed meson mass. On the other hand, within the tetraquark approach, for instance, in Ref. [38] the $2^{++} - 1^{++}$ is about 80 MeV, which is smaller than the difference given in Eq. (1). A similar conclusion is found for the difference between the first radially excited charmonia 2^{++} and 1^{++} by looking at the results for both the Godfrey-Isgur quark model [1] and the one using a screened potential [42], which are about 30 MeV and 40 MeV, respectively.

Even though only the Belle experiment has reported a signal relevant to the spin-2 partner of the $X(3872)$, such a structure can also be searched for in other ongoing and future experiments, e.g., BESIII and its upgrade, LHCb, and PANDA. Belle II also has plans to search for the X_2 state soon. In line with the current and upcoming experiments that will provide more information about such a structure, it is crucial to extend the theoretical studies surveying the X_2 system. In other words, we should further explore the 2^{++} tensor state to help discriminate the various multiquark models used to describe the X_2 structure.

The decays of a 2^{++} tensor structure have been studied in Refs. [44, 45]. In particular, considering that state as the first radial excitation of the P -wave χ_{c2} (2^3P_2) charmonium, the quark model adopted in Ref. [44, 45] provides width estimates for the X_2 decay to charmed mesons around tens of MeV. Moreover, the hadronic decays of the $D^*\bar{D}^*$ S -wave hadronic molecule, into $D\bar{D}$ and $D\bar{D}^*$ meson pairs were estimated to be of the order of a few MeV in Ref. [27] and can be as large as

50 MeV in Ref. [28].

Furthermore, the $X_2 \rightarrow \gamma D\bar{D}^*$ decay width was also calculated in Ref. [27] to be of the keV order. In contrast to the hadronic decays that, according to Ref. [27], has a strong dependence on the ultraviolet (UV) form factors and therefore are sensitive to the short-distance details, radiative decays into $\gamma D\bar{D}^*$ are more sensitive to the long-distance structure of the resonance. Thus, as argued in Ref. [27], one can extract valuable information about the X_2 wave function, as well as about $D\bar{D}^*$ interactions, by surveying such decays. It is not difficult to understand this feature. In the $(D^*\bar{D}^*) \rightarrow \gamma DD^*$ process, the final state receives leading contribution from the one-body transition $D^* \rightarrow D\gamma$, which has no direct relation to the two-body interaction accounting for the short-distance part of the X_2 state. Therefore, the long-range structure of X_2 that determines its coupling to $D^*\bar{D}^*$ has an essential role in its radiative decay into $\gamma D\bar{D}^*$.

Additional interesting decay modes of the X_2 which have not been explored before include the radiative decays into $\gamma\psi(2S)$ and $\gamma J/\psi$ channels. Such a study may help to discriminate the X_2 nature from the $c\bar{c}$ meson $\chi_{c2}(2P)$ possibility. As discussed in, e.g., Ref. [46], the radiative decay matrix element is proportional to the overlap between the wave functions corresponding to the initial and final states. Specifically, for transitions between two charmonia, that overlap is influenced by the position of the nodes of the wave function. Hence, the one-node wave function for the $\psi(2S)$ state has an overlap with the $\chi_{c2}(2P)$ larger than that for the J/ψ one, which is nodeless, such that the following ratio

$$R_{X_2} \equiv \frac{\text{Br}(X_2 \rightarrow \gamma\psi(2S))}{\text{Br}(X_2 \rightarrow \gamma J/\psi)}, \quad (2)$$

should be much larger than the one if the initial particle is the $\chi_{c2}(2P)$ charmonium. Table I shows some results for R_{X_2} obtained in different quark models [44, 45]. Therefore, to confront these results, we evaluate the X_2 radiative decays into $\gamma\psi(2S)$ and $\gamma J/\psi$, assuming that the X_2 resonance is a $D^*\bar{D}^*$ molecular partner of the $X(3872)$ state, predicted in Refs. [17, 23] according to heavy quark spin symmetry (HQSS).

In order to calculate those radiative decay widths, we employ the couplings of the ψ mesons to charmed mesons respecting HQSS and the magnetic and electric couplings of charmed mesons and a photon. The nonrelativistic effective field theory is applied to depict the coupling of the X_2 to $D^*\bar{D}^*$, which is related to the binding energy of X_2 . After calculating the radiative decay widths for $X_2 \rightarrow \psi\gamma$ with $\psi = J/\psi, \psi(2S)$, the upper limit of the ratio R_{X_2} is predicted with the use of the experimental result reported by the BESIII collaboration $R_{X(3872)} < 0.59$ at 90% confidence level [47], and the results for the radiative decays of $X(3872)$ in the hadronic molecular picture [46].

TABLE I. Some results for the radiative decays of the 2^3P_2 charmonium calculated with quark model. Γ_ψ denotes the decay width for $2^3P_2 \rightarrow \gamma\psi$ with $\psi = J/\psi, \psi(2S)$.

	$\Gamma_{J/\psi}$ [keV]	$\Gamma_{\psi(2S)}$ [keV]	R_{X_2}
Ref. [44]	53	207	3.9
Ref. [45]	81	304	3.8

Taking into account the signal yield of X_2 in the $\gamma\psi(2S)$ invariant mass distribution measured by Belle [35], and the predicted upper bound of R_{X_2} , we also estimate the lower limit of the signal yield of X_2 in the $\gamma J/\psi$ mode via the two-photon process at Belle, with J/ψ reconstructed in lepton-antilepton pairs.

The structure of the paper is as follows. In Section II, we discuss the interaction Lagrangians and the main parameters used as well as the relevant Feynman diagrams contributing to the decay process $X_2 \rightarrow \gamma\psi$. The radiative decay ratio R_{X_2} and the signal yield of X_2 in the $\gamma J/\psi$ mode are predicted in Section III. A summary is given in Section IV. Finally, in Appendix A, we provide an update for the results corresponding to the radiative decay widths for $X(3872) \rightarrow \gamma\psi$ discussed in Ref. [46].

II. FORMALISM

A. The Lagrangian and vertices

As discussed in Refs. [48–50] hadron loops play an important role in certain hadron transitions. For pure hadronic molecules, those loops are the leading order contribution to the corresponding transition amplitudes due to the large coupling of the molecule to its constituents. In our case, the X_2 radiative decays under consideration proceeds through the loops depicted in Fig. 1. In order to evaluate each diagram displayed in Fig. 1, we need first to define the interaction Lagrangian that describes all the vertices involved in such loops. We start by the $X_2 D^* \bar{D}^*$ interaction vertex that is described by the following Lagrangian

$$\mathcal{L}_{X_2} = \chi_{\text{nr}}^0 X_2^\dagger{}_{\mu\nu} D^{*0\mu} \bar{D}^{*\nu} + \chi_{\text{nr}}^c X_2^\dagger{}_{\mu\nu} D^{*+\mu} D^{*-\nu} + \text{h.c.}, \quad (3)$$

where χ_{nr}^0 and χ_{nr}^c are the X_2 couplings to the neutral (0) and charged (c) charmed mesons, while the subscript “nr” stands for “nonrelativistic”. As we know, there is a slight difference between the neutral and charged meson masses that leads to an isospin-breaking effect. However, according

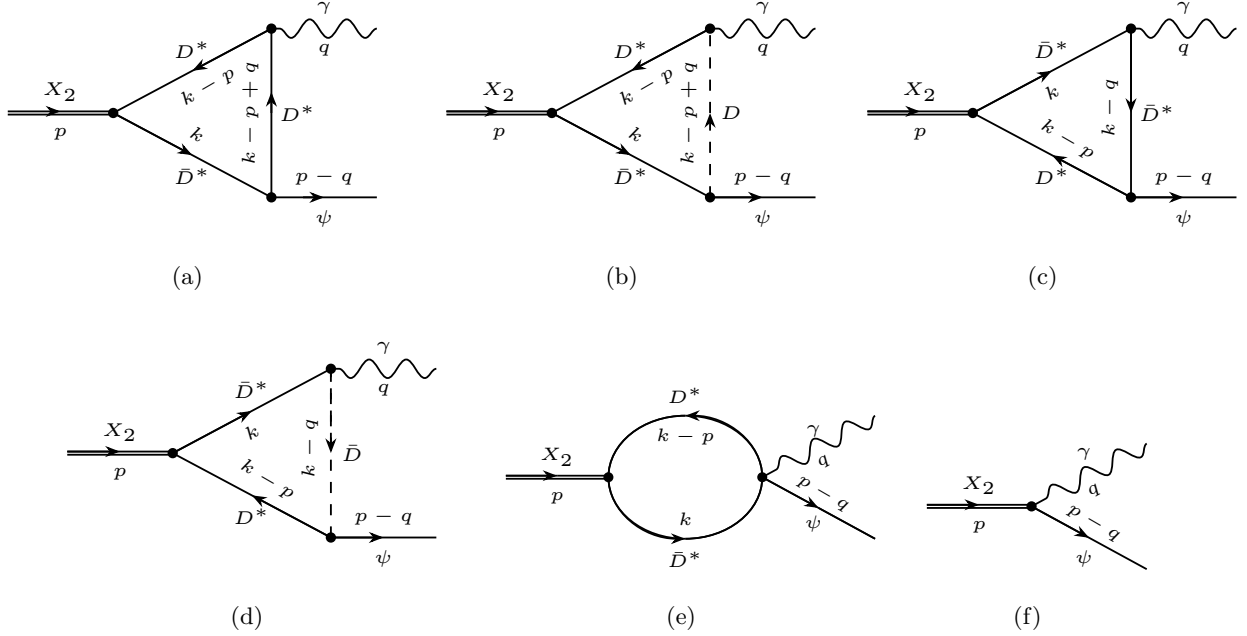


FIG. 1. Feynman diagrams for $X_2 \rightarrow \gamma\psi$ ($\psi = J/\psi, \psi(2S)$).

to Refs. [17, 27], this effect is small so that the couplings χ_{nr}^0 and χ_{nr}^c are approximately the same. In addition, the relative size of X_2 is much smaller compared to the Bohr radius of a ground-state hadronic atom, made out of the charged D^{*+} and D^{*-} mesons, so that the electromagnetic effects can be ignored in such a scenario. Therefore, we follow Ref. [46] and set $\chi_{\text{nr}}^0 = \chi_{\text{nr}}^c = \chi_{\text{nr}}$. The $X_2 D^* \bar{D}^*$ vertex is then

$$\Gamma_{\mu\nu\alpha\beta}^{X_2} = i\chi_{\text{nr}} g_{\mu\alpha} g_{\nu\beta}. \quad (4)$$

Next, the interaction vertex between the ψ and charmed $D^{(*)}$ and $\bar{D}^{(*)}$ mesons can be extracted from

$$\begin{aligned} \mathcal{L}_\psi = & g_2 \psi_\mu \left(\bar{D}^{*\dagger\nu} \overleftrightarrow{\partial}_\nu D^{*\dagger\mu} + \bar{D}^{*\dagger\mu} \overleftrightarrow{\partial}_\nu D^{*\dagger\nu} - \bar{D}^{*\dagger\nu} \overleftrightarrow{\partial}^\mu D^{*\dagger}_\nu \right) - g_2 \psi_\mu \bar{D}^\dagger \overleftrightarrow{\partial}^\mu D^\dagger \\ & - ig_2 \epsilon^{\mu\nu\alpha\beta} \psi_\mu v_\alpha \left(\bar{D}^{*\dagger}_\nu \overleftrightarrow{\partial}_\beta D^\dagger - \bar{D}^\dagger \overleftrightarrow{\partial}_\beta D^{*\dagger}_\nu \right) + \text{h.c.}, \end{aligned} \quad (5)$$

encoding HQSS [51, 52]. In Eq. (5), v_α is the four-velocity of the charmed meson. By defining the four-momentum as $p_\alpha = m_{D^{(*)}} v_\alpha + k_\alpha$, with k_α a residual momentum of $\mathcal{O}(\Lambda_{\text{QCD}})$, and recalling that $v^2 = 1$, we can write v_α as

$$v_\alpha = \frac{p_\alpha}{m_{D^{(*)}}} - \mathcal{O}\left(\frac{k_\alpha}{m_{D^{(*)}}}\right), \quad (6)$$

where $m_{D^{(*)}}$ is the charmed meson mass. Furthermore, we can write the coupling constant g_2 in

terms of the relativistic couplings $g_{D\bar{D}}$, $g_{D\bar{D}^*}$, and $g_{D^*\bar{D}^*}$ as given in Refs. [46, 49, 52], that is

$$g_{\bar{D}D} = g_2 m_D \sqrt{m_\psi}, \quad g_{\bar{D}^*D} = 2g_2 \sqrt{\frac{m_D m_\psi}{m_{D^*}}}, \quad g_{\bar{D}^*D^*} = g_2 m_{D^*} \sqrt{m_\psi}, \quad (7)$$

where m_ψ is the mass of the ψ meson. From Eq. (5) we extract the interaction vertices $\psi_\mu(p) \rightarrow \bar{D}_\nu^*(k_1)D(-k_2)$ and $\psi_\mu(p) \rightarrow \bar{D}_\alpha^*(k_1)D_\beta^*(-k_2)$, which are

$$\Gamma_{\mu\nu}^{(\bar{D}^*D)} = -i \frac{2g_2}{m_{D^*}} \epsilon_{\mu\nu\alpha\beta} k_1^\alpha k_2^\beta, \quad (8)$$

$$\Gamma_{\mu\alpha\beta}^{(\bar{D}^*D^*)} = g_2 [(k_1 + k_2)_\alpha g_{\mu\beta} + (k_1 + k_2)_\beta g_{\mu\alpha} - (k_1 + k_2)_\mu g_{\alpha\beta}]. \quad (9)$$

Now, we move on to the interaction between the charmed mesons and the photon. In this case, we have two couplings corresponding to the electric and magnetic interactions. The former is obtained by gauging the kinetic term associated with the charged $D^{(*)}$ mesons, which is

$$\begin{aligned} \mathcal{L}_e = & \partial_\mu D^\dagger \partial^\mu D - m_D^2 D^\dagger D + ieQ_{D^*} A_\mu (\partial^\mu D^\dagger D - D^\dagger \partial^\mu D) + e^2 Q_{D^*}^2 A_\mu A^\mu D^\dagger D - \frac{1}{2} D_{\mu\nu}^{*\dagger} D^{*\mu\nu} \\ & + m_{D^*}^2 D_\mu^{*\dagger} D^{*\mu} + ieQ_{D^*} A_\mu (D_\nu^{*\dagger} \overleftrightarrow{\partial}^\mu D^{*\nu} + \partial_\nu D^{*\dagger\mu} D^{*\nu} - D^{*\dagger\nu} \partial_\nu D^{*\mu}) \\ & - e^2 Q_{D^*}^2 (A_\mu A^\mu D_\nu^{*\dagger} D^{*\nu} - A_\mu A_\nu D^{*\dagger\nu} D^{*\mu}), \end{aligned} \quad (10)$$

with $eQ_{D^{(*)}}$ standing for the electric charge of the heavy $D^{(*)}$ meson, and $D_{\mu\nu}^* = \partial_\mu D_\nu^* - \partial_\nu D_\mu^*$. The $D_\mu^{*\pm}(k_1) \rightarrow D_\alpha^{*\pm}(k_2)\gamma_\beta(q)$ vertex reads

$$\Gamma_{\mu\alpha\beta}^{(e)} = ie|Q_{D^*}| [(k_1 + k_2)_\beta g_{\mu\alpha} - k_{1\alpha} g_{\mu\beta} - k_{2\mu} g_{\alpha\beta}]. \quad (11)$$

Note that this vertex satisfies the Ward-Takahashi identity, as discussed in Ref. [46]. Besides, after gauging the vertex of Eq. (9), a four-point vertex for $\psi_\mu(p)\gamma_\nu(q) \rightarrow D_\alpha^{*-}(k_1)D_\beta^{*+}(-k_2)$, see the diagram in Fig. 1 (e), reads

$$\Gamma_{\mu\nu\alpha\beta}^{(e)} = 2e|Q_{D^*}| g_2 (g_{\mu\beta} g_{\nu\alpha} + g_{\mu\alpha} g_{\nu\beta} - g_{\mu\nu} g_{\alpha\beta}). \quad (12)$$

On the other hand, the magnetic vertices are extracted from the Lagrangian [53]

$$\begin{aligned} \mathcal{L}_m = & -ieF^{\mu\nu} (D_\mu^{*\dagger} D_\nu^* - D_\nu^{*\dagger} D_\mu^*) \left(\frac{Q\beta'}{2} - \frac{Q'}{2m_c} \right) + e\epsilon^{\mu\nu\alpha\beta} F_{\mu\nu} v_\alpha (D^\dagger D_\beta^* + D_\beta^{*\dagger} D) \left(\frac{Q\beta'}{2} + \frac{Q'}{2m_c} \right) \\ & + ieF^{\mu\nu} (\bar{D}_\mu^{*\dagger} \bar{D}_\nu^* - \bar{D}_\nu^{*\dagger} \bar{D}_\mu^*) \left(\frac{Q\beta'}{2} - \frac{Q'}{2m_c} \right) + e\epsilon^{\mu\nu\alpha\beta} F_{\mu\nu} v_\alpha (\bar{D}^\dagger \bar{D}_\beta^* + \bar{D}_\beta^{*\dagger} \bar{D}) \left(\frac{Q\beta'}{2} + \frac{Q'}{2m_c} \right), \end{aligned} \quad (13)$$

where $Q = \text{Diag}(2/3, -1/3)$ is the light quark charge matrix, and $Q' = 2/3$ corresponds to the charge of the charm quark, while the $F_{\mu\nu}$ stands for the electromagnetic field tensor. In addition, m_c

is the charm quark mass, and the parameter β' is discussed in Ref. [54]. From Eq. (13) the vertices $D_\mu^*(k_1) \rightarrow \gamma_\nu(q)D(k_2)$, $D_\mu^*(k_1) \rightarrow \gamma_\beta(q)D_\alpha^*(k_2)$, $\bar{D}_\mu^*(k_1) \rightarrow \gamma_\nu(q)\bar{D}(k_2)$ and $\bar{D}_\mu^*(k_1) \rightarrow \gamma_\beta(q)\bar{D}_\alpha^*(k_2)$ are

$$\Gamma_{\mu\nu}^{(m)D^*D\gamma} = e\epsilon_{\mu\nu\alpha\beta}v_\alpha q_\beta \left(\beta'Q + \frac{Q'}{m_c} \right), \quad (14)$$

$$\Gamma_{\mu\alpha\beta}^{(m)D^*D^*\gamma} = ie(q_\alpha g_{\mu\beta} - q_\mu g_{\alpha\beta}) \left(\beta'Q - \frac{Q'}{m_c} \right), \quad (15)$$

$$\Gamma_{\mu\nu}^{(m)\bar{D}^*\bar{D}\gamma} = e\epsilon_{\mu\nu\alpha\beta}v_\alpha q_\beta \left(\beta'Q + \frac{Q'}{m_c} \right), \quad (16)$$

$$\Gamma_{\mu\alpha\beta}^{(m)\bar{D}^*\bar{D}^*\gamma} = -ie(q_\alpha g_{\mu\beta} - q_\mu g_{\alpha\beta}) \left(\beta'Q - \frac{Q'}{m_c} \right). \quad (17)$$

As in Eq. (11), these vertices also satisfy the appropriate Ward identity.

B. The amplitude $X_2 \rightarrow \gamma\psi$

Once we have all the vertices in the loop diagrams in Fig. 1, we are able to write the amplitude for the $X_2 \rightarrow \gamma\psi$ decay. Namely,

$$i\mathcal{M} = ie\chi_{\text{nr}}g_2\epsilon^{*\mu\nu}(X_2)\epsilon^\beta(\gamma)\epsilon^\sigma(\psi)\mathcal{M}_{\mu\nu\beta\sigma}, \quad (18)$$

with $\epsilon^{*\mu\nu}(X_2)$, $\epsilon^\beta(\gamma)$, and $\epsilon^\sigma(\psi)$ the polarization vectors for the X_2 state, the photon, and ψ mesons (ψ' , and J/ψ), respectively. The tensor structure $\mathcal{M}_{\mu\nu\beta\sigma}$ in Eq. (18) encodes the contributions of all the diagrams in Fig. 1, and it is written as

$$\mathcal{M}_{\mu\nu\beta\sigma} = \sqrt{m_{X_2}m_\psi} \int \frac{d^4k}{(2\pi)^4} S_\nu^\rho(k) S_\mu^\alpha(k-p) \left(J_{\alpha\rho\beta\sigma}^{(a)m}(k) + J_{\alpha\rho\beta\sigma}^{(a)e}(k) + J_{\alpha\rho\beta\sigma}^{(b)m}(k) + J_{\alpha\rho\beta\sigma}^{(c)m}(k) + J_{\alpha\rho\beta\sigma}^{(c)e}(k) + J_{\alpha\rho\beta\sigma}^{(d)m}(k) + J_{\alpha\rho\beta\sigma}^{(e)e}(k) \right), \quad (19)$$

where the superscripts (a)-(e) match the labels of each individual diagram in Fig. 1. Yet, the contributions in Eq. (19) with the labels m and e corresponds to the magnetic and electric couplings, respectively. Explicitly, each contribution in Eq. (19) reads

$$J_{\alpha\rho\beta\sigma}^{(a)m}(k) = \frac{i}{3}m_{D^*}^3 S^{\xi\gamma}(k-p+q) [(2k-p+q)_\sigma g_{\rho\xi} - (2k-p+q)_\rho g_{\sigma\xi} - (2k-p+q)_\xi g_{\rho\sigma}] (q_\alpha g_{\gamma\beta} - q_\gamma g_{\alpha\beta}) \left(\beta' - \frac{4}{m_c} \right), \quad (20)$$

$$J_{\alpha\rho\beta\sigma}^{(a)e}(k) = im_{D^*}^2 S^{\xi\gamma}(k-p+q) [(2k-p+q)_\sigma g_{\rho\xi} - (2k-p+q)_\rho g_{\sigma\xi} - (2k-p+q)_\xi g_{\rho\sigma}] [(2k-2p+q)_\beta g_{\alpha\gamma} - (k-p+q)_\alpha g_{\gamma\beta} - (k-p)_\gamma g_{\alpha\beta}], \quad (21)$$

$$J_{\alpha\rho\beta\sigma}^{(b)m}(k) = -\frac{2i}{3}m_{D^*}S(k-p+q)\epsilon_{\sigma\rho\gamma\delta}k^\gamma(k-p+q)^\delta\epsilon_{\alpha\beta\xi\eta}(k-p)^\xi q^\eta\left(\beta' + \frac{4}{m_c}\right), \quad (22)$$

$$J_{\alpha\rho\beta\sigma}^{(c)m}(k) = -\frac{i}{3}m_{D^*}^3S^{\xi\gamma}(k-q)[(2k-p-q)_\sigma g_{\alpha\xi} - (2k-p-q)_\xi g_{\sigma\alpha} - (2k-p-q)_\alpha g_{\sigma\xi}] \\ (q_\gamma g_{\rho\beta} - q_\rho g_{\beta\gamma})\left(\beta' - \frac{4}{m_c}\right), \quad (23)$$

$$J_{\alpha\rho\beta\sigma}^{(c)e}(k) = im_{D^*}^2S^{\xi\gamma}(k-q)[(2k-p-q)_\sigma g_{\alpha\xi} - (2k-p-q)_\xi g_{\sigma\alpha} - (2k-p-q)_\alpha g_{\sigma\xi}] \\ [(2k-q)_\beta g_{\rho\gamma} - k_\gamma g_{\rho\beta} - (k-q)_\rho g_{\gamma\beta}], \quad (24)$$

$$J_{\alpha\rho\beta\sigma}^{(d)m}(k) = \frac{2i}{3}m_D S(k-q)\epsilon_{\rho\beta\xi\eta}k^\xi q^\eta\epsilon_{\sigma\alpha\gamma\delta}(k-q)^\gamma(k-p)^\delta\left(\beta' + \frac{4}{m_c}\right), \quad (25)$$

$$J_{\alpha\rho\beta\sigma}^{(e)}(k) = 2m_{D^*}^2(g_{\alpha\sigma}g_{\beta\rho} + g_{\sigma\rho}g_{\alpha\beta} - g_{\alpha\rho}g_{\beta\sigma}), \quad (26)$$

with S and $S_{\mu\nu}$ the propagator for the heavy fields D and D^* , respectively, given by

$$S(\tilde{p}) = \frac{i}{\tilde{p}^2 - m_D^2 + i\epsilon}, \\ S_{\mu\nu}(\tilde{p}) = \frac{i}{\tilde{p}^2 - m_{D^*}^2 + i\epsilon}\left(-g_{\mu\nu} + \frac{\tilde{p}_\mu\tilde{p}_\nu}{m_{D^*}^2}\right). \quad (27)$$

The factor $\sqrt{m_{X_2}m_\psi}$ in Eq. (19) accounts for the normalization of the heavy meson fields.² It is worth noticing that, as a consistency check, the loop amplitude in Eq. (19) is gauge invariant, as we must expect.

The loop amplitude defined in Eq. (19) is a UV divergent integral. In order to have a well-defined amplitude from which we can get consistent results, we add a $X_2\gamma\psi$ counterterm amplitude like the case for the $X(3872) \rightarrow \gamma\psi$ [46], depicted in Fig. 1(f), to the one given in Eq. (19). Specifically, it is

$$i\mathcal{M}^{\text{cont}} = i\lambda_1\epsilon_{\mu\nu}^*(X_2)\epsilon^\mu(\gamma)\epsilon^\nu(\psi) + i\lambda_2q^\mu q^\nu\epsilon_{\mu\nu}^*(X_2)p \cdot \epsilon(\gamma)q \cdot \epsilon(\psi) \\ + i\lambda_3q^\mu\epsilon^\nu(\psi)\epsilon_{\mu\nu}^*p \cdot \epsilon(\gamma) + i\lambda_4q^\mu\epsilon^\nu(\gamma)\epsilon_{\mu\nu}^*p \cdot \epsilon(\psi) + i\lambda_5q^\mu q^\nu\epsilon_{\mu\nu}^*\epsilon(\gamma) \cdot \epsilon(\psi), \quad (28)$$

which is straightforward to see its manifest gauge invariance. These terms are defined such that λ_r ($r = 1, \dots, 5$), which is subject to renormalization, absorbs the UV divergence from the loops in Eq. (19), as done in Ref. [46]. On the one hand, the counterterm defined in Ref. [46] has only one parameter λ ; on the other hand, in our case, Eq. (28) has five terms with each one having its strength λ_r . However, for our purposes, we do not consider relations among them.

² Except for the electric coupling in Eq. (11), we use the nonrelativistic normalization for the heavy mesons (including the charmonium, charmed mesons, and X_2), which differs from the traditional relativistic normalization by a factor $\sqrt{m_H}$.

The $X_2 \rightarrow \gamma\psi$ two-body decay width is given by the following formula

$$\begin{aligned}\Gamma_{X_2} &= e^2 \chi_{\text{nr}}^2 g_2^2 \sum_{\text{polarizations}} \frac{1}{5} \frac{q}{8\pi m_{X_2}^2} \left| \epsilon^{*\mu\nu}(X_2) \epsilon^\beta(\gamma) \epsilon^\sigma(\psi) \mathcal{M}_{\mu\nu\beta\sigma} \right|^2 \\ &= - \frac{e^2 \chi_{\text{nr}}^2 g_2^2 q}{40\pi m_{X_2}^2} \mathcal{M}_{\mu\nu\beta\sigma} \mathcal{M}_{\mu'\nu'\beta'\sigma'}^* \bar{g}^{\sigma\sigma'}(p-q, m_\psi) g^{\beta\beta'} P^{(2)\mu\nu\mu'\nu'}(p, m_{X_2}),\end{aligned}\quad (29)$$

where $q = |\vec{q}|$ stands for the momentum of the final states (γ or ψ) in the center-of-mass frame,

$$q = \frac{m_{X_2}^2 - m_\psi^2}{2m_{X_2}}.\quad (30)$$

Furthermore, $P_{\mu\nu\mu'\nu'}^{(2)}(p, m_{X_2})$ in Eq. (29) is the projection operator corresponding to the summation over the polarizations of X_2 , which is given by [55]

$$\begin{aligned}P_{\mu\nu\mu'\nu'}^{(2)}(p, m_{X_2}) &= \sum_{\text{polarizations}} \epsilon_{\mu\nu}(p, m_{X_2}) \epsilon_{\mu'\nu'}(p, m_{X_2}) \\ &= \frac{1}{2} [\bar{g}_{\mu\mu'}(p, m_{X_2}) \bar{g}_{\nu\nu'}(p, m_{X_2}) + \bar{g}_{\mu\nu'}(p, m_{X_2}) \bar{g}_{\nu\mu'}(p, m_{X_2})] \\ &\quad - \frac{1}{3} \bar{g}_{\mu\nu}(p, m_{X_2}) \bar{g}_{\mu'\nu'}(p, m_{X_2}),\end{aligned}\quad (31)$$

where $\bar{g}_{\alpha\beta}$ denotes the summation over the polarization vectors

$$\bar{g}_{\alpha\beta}(p, m) = -g_{\alpha\beta} + \frac{p_\alpha p_\beta}{m^2},\quad (32)$$

with four-momentum p and mass m .

In the next subsection, we shall discuss the parameters used in our numerical analysis, which will be presented later in Section III.

C. The parameters

In order to numerically calculate the radiative decay widths of X_2 , we should fix the values for the parameters used. The values for the meson masses are [43]

$$m_D = 1867.25 \text{ MeV}, \quad m_{D^*} = 2008.56 \text{ MeV}, \quad m_{X_2} = 4014.3 \text{ MeV},$$

$$m_{J/\psi} = 3096.90 \text{ MeV}, \quad m_{\psi(2S)} = 3686.10 \text{ MeV},$$

where m_D (m_{D^*}) is the average mass between the neutral and charged D (D^*) mesons, and the X_2 mass is taken from Ref. [35]. The charm quark mass and the parameter related to the magnetic coupling are fixed by the partial electromagnetic widths for $D^{*0} \rightarrow \gamma D^0$ and $D^{*+} \rightarrow \gamma D^+$ [54],

$$\beta'^{-1} = 379 \text{ MeV}, \quad m_c = 1863 \text{ MeV}.\quad (33)$$

The coupling constant for X_2 to the charged and neutral charmed mesons is extracted from the binding energy of X_2 [56, 57],

$$\chi_{\text{nr}}^0 = \left\{ \lambda^2 \frac{16\pi}{\mu_{*0}} \sqrt{\frac{2E_B}{\mu_{*0}}} \left[1 + \mathcal{O}(\sqrt{2\mu_{*0}E_B r}) \right] \right\}^{1/2}, \quad (34)$$

where E_B and μ_{*0} are the binding energy of X_2 relative to the $D^{*0}\bar{D}^{*0}$ threshold and the $D^{*0}\bar{D}^{*0}$ reduced mass, respectively. r is identified with the range of forces, where $1/r \gg \sqrt{2\mu_{*0}E_B}$ in the weak binding limit [58]. We assume that the X_2 is a pure $D^*\bar{D}^*$ bound state, $\lambda^2 = 1$, and then we obtain the coupling constant $\chi_{\text{nr}} = 1.3_{-1.3}^{+1.0} \text{ GeV}^{-1/2}$, where the uncertainty is derived from the uncertainties of D^{*0} (\bar{D}^{*0}) and X_2 masses. Besides, g and g' denote the J/ψ and $\psi(2S)$ couplings to the charmed mesons, respectively.

We evaluate the loop integrals in Fig. 1 by using the dimensional regularization method. In particular, we adopt the $\overline{\text{MS}}$ subtraction scheme. As for the strength of the interaction corresponding to the counterterms, denoted by the λ_r parameters, following the idea in Ref. [46], we set to zero the contribution of the finite part of the counterterms in Eq. (28) and vary the energy scale in a large range, 1.5–7.0 GeV, in the UV divergent loop integrals. We define the ratios

$$r_\chi \equiv \left| \frac{\chi_{\text{nr}}}{\bar{\chi}_{\text{nr}}} \right|, \quad r'_\chi \equiv \left| \frac{\chi'_{\text{nr}}}{\bar{\chi}'_{\text{nr}}} \right|, \quad r_g \equiv \left| \frac{g_2}{g_2^0} \right|, \quad r'_g \equiv \left| \frac{g'_2}{g_2^0} \right|, \quad (35)$$

where g_2 (g'_2) is the coupling constant between J/ψ ($\psi(2S)$) and charmed mesons in Eq. (7). We take $\bar{\chi}_{\text{nr}} = 1.3 \text{ GeV}^{-1/2}$ and $g_2^0 = 2.0 \text{ GeV}^{-3/2}$ with the latter from the model-dependent estimates discussed in Refs. [49, 52]. The $X(3872)$ coupling to $D\bar{D}^*$ is denoted as χ'_{nr} , and its benchmark value is set to $\bar{\chi}'_{\text{nr}} = 0.97 \text{ GeV}^{-1/2}$ [59].

In what follows, we present the numerical results for the X_2 radiative decays into $\gamma\psi$. In order to perform the numerical analysis, we have used the following Mathematica packages: FeynCalc [60], FeynHelpers [61], and Package-X [62].

III. NUMERICAL RESULTS

In Table II, we show our numerical results for the partial decays $X_2 \rightarrow \gamma\psi$ with $\psi = \psi(2S)$ and J/ψ as given in Eq. (29), along with the corresponding ratio R_{X_2} . These observables depend on the products among the quantities defined in Eq. (35). In order to fix those quantities, we have to make assumptions on the coupling constants g_2 and g'_2 since their values are not well established in the literature. Besides, we have also to fix the contribution from the contact terms, that is, to fix the size of λ_r 's in Eq. (28), which is unknown; however, as discussed Ref. [46], we may estimate

their size by noticing that any change in μ must also change the counterterms accordingly so that the overall result does not depend on the renormalization scale μ . Thus, we set $\lambda_r = 0$ and vary the scale μ within a large range from 1.5 GeV up to $2m_{X_2}$, with m_{X_2} the X_2 mass, as mentioned above. In Table II, we can see such behavior in the partial decays under consideration by noticing their corresponding changes as μ varies. In other words, such variation in each partial decay width we are concerned with may be considered a measure of the size of λ_r 's.

TABLE II. Decay widths and their ratio R for the process $X \rightarrow \gamma\psi$ with $X = X(3872), X_2$ and $\psi = J/\psi, \psi(2S)$. Γ'_ψ and Γ_ψ denote the decay width for $X(3872) \rightarrow \psi\gamma$ and $X_2 \rightarrow \psi\gamma$, respectively. The first row is the energy scale in the $\overline{\text{MS}}$ subtraction scheme, g_2 (g'_2) is the coupling constant in Eq. (7), and r'_χ, r_g , and r'_g are defined in Eq. (35). In the last row, $N_{\min}(X_2 \rightarrow \gamma J/\psi)$ denotes the lower limit of the X_2 signal yield in the $J/\psi\gamma \rightarrow \ell^+\ell^-\gamma$ ($\ell = e, \mu$) mode for the two-photon process at Belle.

μ (GeV)	1.5	2.0	4.0	7.0
$\Gamma'_{J/\psi}$ (keV)	162 $(r'_\chi r_g)^2$	176 $(r'_\chi r_g)^2$	212 $(r'_\chi r_g)^2$	244 $(r'_\chi r_g)^2$
$\Gamma'_{\psi(2S)}$ (keV)	17.5 $(r'_\chi r'_g)^2$	18.4 $(r'_\chi r'_g)^2$	20.8 $(r'_\chi r'_g)^2$	22.7 $(r'_\chi r'_g)^2$
$\Gamma_{J/\psi}$ (keV)	139 $(r_\chi r_g)^2$	161 $(r_\chi r_g)^2$	224 $(r_\chi r_g)^2$	284 $(r_\chi r_g)^2$
$\Gamma_{\psi(2S)}$ (keV)	25.0 $(r_\chi r'_g)^2$	27.1 $(r_\chi r'_g)^2$	32.7 $(r_\chi r'_g)^2$	37.6 $(r_\chi r'_g)^2$
$R_{X(3872)}$	0.11 $(g'_2/g_2)^2$	0.10 $(g'_2/g_2)^2$	0.10 $(g'_2/g_2)^2$	0.09 $(g'_2/g_2)^2$
R_{X_2}	0.18 $(g'_2/g_2)^2$	0.17 $(g'_2/g_2)^2$	0.15 $(g'_2/g_2)^2$	0.13 $(g'_2/g_2)^2$
$R_{X_2}/R_{X(3872)}$	1.67	1.61	1.49	1.43
$N_{\min}(X_2 \rightarrow \gamma J/\psi)$	35	36	39	41

As for the ratio R_{X_2} , we set the finite part of the counterterm to zero and R_{X_2} will depend only on the ratio g'_2/g_2 at a given scale. In order to fix this latter ratio, we consider some model-dependent estimates. If g'_2/g_2 is assumed to equal to unity, for the $X(3872)$ case the $\gamma\psi(2S)$ channel is relatively suppressed [46]. Similarly, in our case, by considering $g'_2/g_2 = 1$, we find that the $\gamma\psi(2S)$ channel is also suppressed. In Ref. [63], the ratio was fixed to $g'_2/g_2 = 1.67$ by modeling the couplings in a vector-meson dominance picture [52]; in this case, the $\gamma\psi(2S)$ channel is still suppressed relatively to the $\gamma J/\psi$ channel. Alternatively, we can fix g'_2/g_2 by using the upper limit for the ratio $R_{X(3872)}$ corresponding to the $X(3872) \rightarrow \gamma\psi(2S)$ and $\gamma J/\psi$, reported by BESIII in Ref. [47]. The $X(3872)$ radiative decays are discussed in Ref. [46] (see Appendix A which updates a couple of expressions in Ref. [46]). The results for the $X(3872)$ state are also shown in Table II.

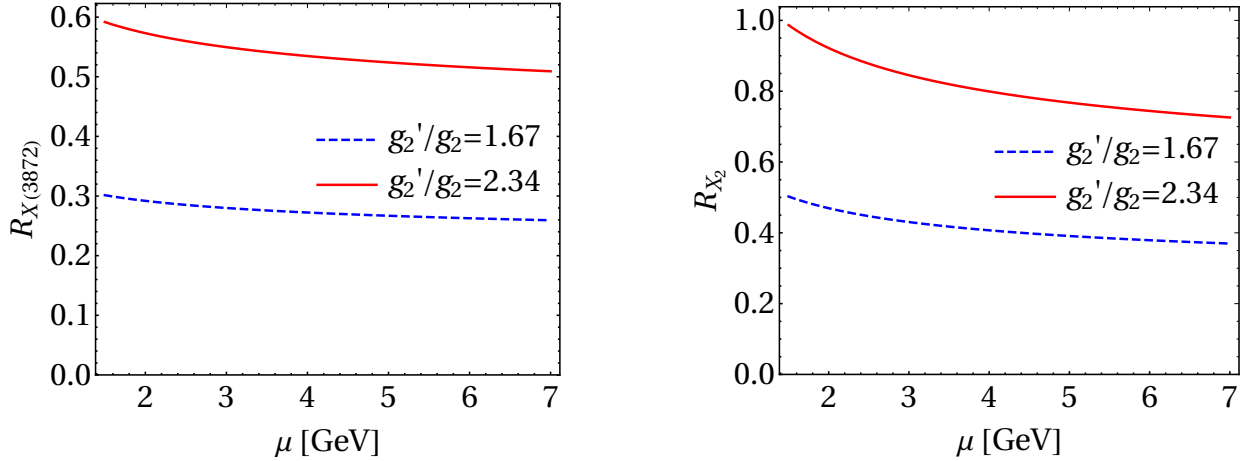


FIG. 2. Scale dependence of the ratios $R_{X(3872)}$ and R_{X_2} , where μ is the energy scale in the $\overline{\text{MS}}$ subtraction scheme of the dimensional regularization method used to regularize the loops in Fig. 1. $g'_2/g_2 = 2.34$ is the upper bound given in Eq. (36), derived from the BESIII measurement $R_{X(3872)} < 0.59$ [47], and $g'_2/g_2 = 1.67$ is the model value used in Ref. [63].

Note that, in this case, the $R_{X(3872)}$ barely changes as we vary the scale μ . Thus, we can choose one specific value for μ , for instance, $\mu = 1.5$ GeV, and then, by using the BESIII measurement for $R_{X(3872)} < 0.59$, we obtain from Table II

$$g'_2/g_2 < 2.34. \quad (36)$$

As a matter of checking, in Fig. 2, we show the plots for both ratios $R_{X(3872)}$ and R_{X_2} as a function of the scale μ . As we can see, within the range $1.5 \text{ GeV} \leq \mu \leq 2m_{X_2}$, those ratios are, to a good approximation, independent of μ , as we expect.

As discussed above, both ratios $R_{X(3872)}$ and R_{X_2} depend on g'_2/g_2 value, whose value is not fixed and model dependent. However, we can determine R_{X_2} independently of the couplings g'_2 and g_2 , using the experimental information for $R_{X(3872)} < 0.59$, measured by BESIII in Ref. [47], as an input. Specifically, in Fig. 3 we show the double ratio $R_{X_2}/R_{X(3872)}$ as a function of μ . Note that this observable only slightly decreases from 1.67 to 1.43 as the renormalization scale μ varies within the large range $[1.5 \text{ GeV}, 2m_{X_2}]$. This flat variation indicates that we can set any value within that range for $R_{X_2}/R_{X(3872)}$, and then use the upper boundary $R_{X(3872)} < 0.59$ provided by BESIII such that we obtain an upper limit for R_{X_2} :

$$R_{X_2} \lesssim 1.0. \quad (37)$$

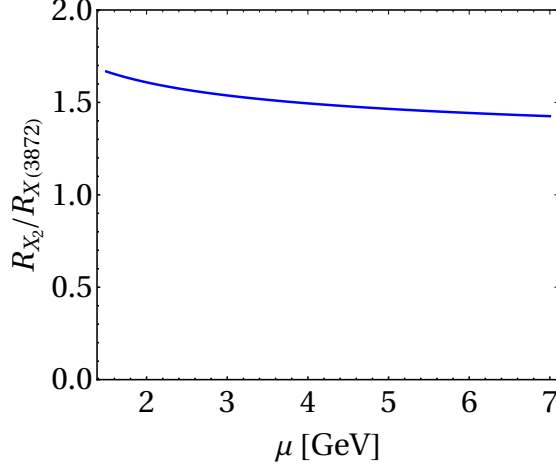


FIG. 3. Scale dependence of the double ratio $R_{X_2}/R_{X(3872)}$.

Next, we shall estimate the number of events of X_2 that can be collected in the $\gamma J/\psi$ final state of the two-photon process at the Belle experiment. The signal yield of X_2 in such a process is given by

$$N(X_2 \rightarrow \gamma\psi) = \Gamma_{\gamma\gamma} \text{Br}[X_2] \text{Br}[\psi] \epsilon F(\sqrt{s}, J) L_{\text{tot}}, \quad (38)$$

where $\Gamma_{\gamma\gamma}$ is the two-photon decay width of X_2 , $\text{Br}[X_2]$ is the branching fraction for $X_2 \rightarrow \gamma\psi$ ($\psi = J/\psi, \psi(2S)$), ϵ is the efficiency, and L_{tot} is the total integrated luminosity of the Belle data sample. In addition, for the $\psi(2S)$ reconstructed from $J/\psi\pi^+\pi^-$ as done in Ref. [35] and J/ψ from the $\ell^+\ell^-$ lepton pairs ($\ell = e, \mu$), one has $\text{Br}[\psi(2S)] = \text{Br}[\psi(2S) \rightarrow \pi^+\pi^- J/\psi] \text{Br}[J/\psi \rightarrow \ell^+\ell^-]$ and $\text{Br}[J/\psi] = \text{Br}[J/\psi \rightarrow \ell^+\ell^-]$. The factor $F(\sqrt{s}, J)$ is related to the two-photon luminosity function $L_{\gamma\gamma}$ [35, 64]

$$F(\sqrt{s}, J) = 4\pi^2(2J+1)L_{\gamma\gamma}(\sqrt{s})/s, \quad (39)$$

with the effective energy of the two-photon collision \sqrt{s} and the spin J for X_2 . Since the two-photon decay width $\Gamma_{\gamma\gamma}$, the efficiency ϵ , the total integrated luminosity L_{tot} and the factor $F(\sqrt{s}, J)$ are the same for $N(X_2 \rightarrow \gamma J/\psi)$ and $N(X_2 \rightarrow \gamma\psi(2S))$, the signal yield of X_2 in the $\gamma J/\psi$ with $J/\psi \rightarrow \ell^+\ell^-$ is given by

$$N(X_2 \rightarrow \gamma J/\psi) = \frac{N(X_2 \rightarrow \gamma\psi(2S))}{R_{X_2} \text{Br}[\psi(2S) \rightarrow \pi^+\pi^- J/\psi]}. \quad (40)$$

The signal yield of X_2 is 19 ± 7 in Ref. [35], and the branching fraction for $\psi(2S) \rightarrow \pi^+\pi^- J/\psi$ is $(34.68 \pm 0.30)\%$ [43]. As discussed above, for $\mu = 1.5$ GeV we have $R_{X_2} \lesssim 1.0$, the yield of X_2 is

$$N(X_2 \rightarrow \gamma J/\psi) \gtrsim 35. \quad (41)$$

Therefore, we estimate that the signal yield of X_2 observed in the $\gamma J/\psi$ invariant mass distribution is at least about 35 for the two-photon collision at Belle. Besides, the minimal yields of X_2 estimated with other energy scales are listed in Table II. The prediction can be checked with the Belle data.

IV. SUMMARY

By assuming the existence of a tensor state X_2 , that, according to HQSS, is a spin partner of the $X(3872)$ state in the hadronic molecular model, as predicted in Refs. [17, 18, 23], we have evaluated its radiative decays into $\gamma\psi(2S)$ and $\gamma J/\psi$ channels. Although with low statistics, a candidate of such a state was recently observed by the Belle Collaboration in Ref. [35], with mass and width in accordance with the corresponding values predicted in Refs. [17, 18, 23].

In particular, in our case, the decays we are concerned with proceed through hadronic loops with charmed mesons as intermediate particles. These loops are UV divergent, requesting an introduction of additional counterterm amplitude, in which the strength of that contact interaction absorbs the infinities after renormalization. However, with the available theoretical information, it is impossible to determine the contribution from the counterterms precisely. Notwithstanding, we estimated their contributions by varying the renormalization scale, as done in Ref. [46] for the $X(3872)$ case, such that the changes in the partial decay widths encode the size of the counterterm.

Moreover, we have used effective Lagrangians to describe the X_2 couplings to the charmed D^* and \bar{D}^* mesons, and the couplings of those mesons with the charmonia $\psi(2S)$ and J/ψ . Since these latter set of couplings are not well-determined in literature, we have written the partial decays $X_2 \rightarrow \gamma\psi(2S)$ and $X_2 \rightarrow \gamma J/\psi$ in terms of ratios involving those couplings, that allows us to draw conclusions based on the relations among them.

According to our findings, for values of g'_2/g_2 close to one, we always find suppression of the $\gamma\psi(2S)$ channel against the $\gamma J/\psi$ one. On the other hand, as g'_2/g_2 increases the ratios $R_{X(3872)}$ and R_{X_2} increase accordingly. We have fixed the range of g'_2/g_2 to be < 2.34 using input from the BESIII measurement of $R_{X(3872)} < 0.59$. Consequently, we found $R_{X_2} \lesssim 1.0$. As a matter of comparison, R_{X_2} estimated using the quark model assuming the X_2 to be the $\chi_{c2}(2P)$ meson leads to a value about 4, as displayed in Table I, significantly larger than the one we obtained in the hadronic molecular picture. In principle, future experimental measurements of the observable R_{X_2} may shed light on the internal structure of X_2 .

Finally, we predict the signal yield of X_2 in the $\gamma J/\psi$ spectrum from the two-photon process based on our findings for R_{X_2} , and also the yields of X_2 in the $\gamma\gamma \rightarrow \gamma\psi(2S)$ reaction reported

by the Belle Collaboration [35]. As a result, we expect that the yield of X_2 in the $\gamma J/\psi \rightarrow \gamma \ell^+ \ell^-$ final states ($\ell = e, \mu$) should be at least about 35, that is larger than the number of events observed by the Belle collaboration in Ref. [35].

ACKNOWLEDGMENTS

We would like to thank Alexey Nefediev for valuable discussions. This work is partly supported by the Chinese Academy of Sciences under Grant No. XDB34030000; by the National Natural Science Foundation of China (NSFC) under Grants No. 12125507, No. 11835015, and No. 12047503; and by the NSFC and the Deutsche Forschungsgemeinschaft (DFG) through the funds provided to the Sino-German Collaborative Research Center ‘‘Symmetries and the Emergence of Structure in QCD’’ (NSFC Grant No. 12070131001, DFG Project-ID 196253076 - TRR110).

Appendix A: $X(3872)$ radiative decays into $\gamma \psi(2S)$ and $\gamma J/\psi$ channels

The $X(3872)$ radiative decays into the $\gamma \psi(2S)$ and $\gamma J/\psi$ channels have been evaluated in Ref. [46], adopting a molecular picture as the quark configuration for the $X(3872)$ state. The findings reported in Ref. [46] are in line with the experimental ratio $R_{X(3872)}$ measured by the BESIII Collaboration [47]. In particular, it is stressed in Ref. [46] that those specific decays take place through hadron loops involving charmed mesons plus short-distance contributions in the form of a counterterm. For pure hadronic molecular states the hadron loops are the leading order contribution and play an important role in such processes. However, the charged conjugated diagrams in the loops are not considered in Ref. [46]; these contributions will lead to a factor of 2 for all the loop contributions but does not affect the ratio $R_{X(3872)}$ which was the main concern in Ref. [46]. In addition, p^α in Eq. (24) and p^γ in Eq. (28) in Ref. [46] should be changed to k^α and $(k-p)^\gamma$, respectively, which has also been noticed in Ref. [30]. That is because the four-velocity of heavy mesons with respect to the magnetic vertices in Eqs. (14) and (16) are related to the charmed-meson momentum inside the loop, instead of the $X(3872)$ four-velocity. The updated expressions of Eqs.(24)-(29) in Ref. [46] for the individual contributions to the process $X_\sigma(p) \rightarrow \gamma_\lambda(q) \psi_\mu(p-q)$ are (we use the same notation as in Ref. [46])

$$J_{\mu\nu\lambda}^{(a)m}(k) = \frac{2}{3}m \left(\beta + \frac{4}{m_c} \right) \epsilon_{\nu\lambda\alpha\beta} k^\alpha q^\beta \frac{(2k-p-q)_\mu}{(k-q)^2 - m^2},$$

$$J_{\mu\nu\lambda}^{(b)e}(k) = 4\epsilon_{\mu\rho\alpha\beta} \frac{(k-p)^\alpha (k-q)^\beta}{(k-q)^2 - m_*^2} [(2k-q)_\lambda g_\nu^\rho - (k-q)_\nu g_\lambda^\rho - k^\rho g_{\nu\lambda}],$$

TABLE III. Decay widths $X(3872) \rightarrow \gamma\psi$ with $\psi = J/\psi, \psi(2S)$ and their ratio $R_{X(3872)}$. The second row displays the results for $X(3872) \rightarrow \gamma\psi$ with $\psi = J/\psi, \psi(2S)$ calculated in Ref. [46], while the updated results are shown in the third row.

	μ	$\Gamma'_{J/\psi}$ [keV]	$\Gamma'_{\psi(2S)}$ [keV]	$R_{X(3872)}$
Ref. [46]	$m_{X(3872)}$	23.5 $(r'_\chi r'_g)^2$	4.9 $(r'_\chi r'_g)^2$	0.21 $(g'_2/g_2)^2$
Updated	$m_{X(3872)}$	211 $(r'_\chi r'_g)^2$	20.6 $(r'_\chi r'_g)^2$	0.10 $(g'_2/g_2)^2$

$$\begin{aligned}
J_{\mu\nu\lambda}^{(b)m}(k) &= \frac{4}{3}m_* \left(\beta - \frac{4}{m_c} \right) \epsilon_{\mu\rho\alpha\beta} \frac{(k-p)^\alpha (k-q)^\beta}{(k-q)^2 - m_*^2} [q_\nu g_\lambda^\rho - q^\rho g_{\nu\lambda}], \\
J_{\mu\nu\lambda}^{(c)e}(k) &= 4\epsilon_{\mu\nu\alpha\beta} (k-p+q)^\alpha k^\beta \frac{(2k-2p+q)_\lambda}{(k-p+q)^2 - m^2}, \\
J_{\mu\nu\lambda}^{(d)m}(k) &= \frac{2}{3}m_* \left(\beta + \frac{4}{m_c} \right) [(2k-p+q)_\mu g_{\beta\nu} - (2k-p+q)_\beta g_{\mu\nu} - (2k-p+q)_\nu g_{\beta\mu}] \frac{\epsilon_{\alpha\lambda\gamma\delta} (k-p)^\gamma q^\delta}{(k-p+q)^2 - m_*^2} \\
&\quad \left(-g^{\alpha\beta} + \frac{(k-p+q)^\alpha (k-p+q)^\beta}{m_*^2} \right), \\
J_{\mu\nu\lambda}^{(e)e}(k) &= -4\epsilon_{\mu\nu\lambda\alpha} p^\alpha, \tag{A1}
\end{aligned}$$

where m and m_* are the masses of D and D^* mesons, respectively, and the magnetic coupling parameter β is the β' in Eq. (33).

The updated numerical results for the partial decay widths of $X(3872) \rightarrow \gamma\psi(2S)$ and $\gamma J/\psi$ are shown in Table III, where we have kept the results from Ref. [46] for a comparison. As can be seen, they are much larger than the ones in Ref. [46]. As for the ratio $R_{X(3872)}$, the new result is about half of the previous one. Nevertheless, the conclusion in Ref. [46], that is the hadronic molecular picture of the $X(3872)$ is compatible with the measured ratio $R_{X(3872)}$, is not altered.

-
- [1] S. Godfrey and N. Isgur, Mesons in a Relativized Quark Model with Chromodynamics, [Phys. Rev. D **32**, 189 \(1985\)](#).
 - [2] H.-X. Chen, W. Chen, X. Liu, and S.-L. Zhu, The hidden-charm pentaquark and tetraquark states, [Phys. Rep. **639**, 1 \(2016\)](#), [arXiv:1601.02092 \[hep-ph\]](#).
 - [3] A. Hosaka, T. Iijima, K. Miyabayashi, Y. Sakai, and S. Yasui, Exotic hadrons with heavy flavors: X, Y, Z , and related states, [Prog. Theor. Exp. Phys. **2016**, 062C01 \(2016\)](#), [arXiv:1603.09229 \[hep-ph\]](#).
 - [4] A. Esposito, A. Pilloni, and A. D. Polosa, Multiquark Resonances, [Phys. Rept. **668**, 1 \(2017\)](#), [arXiv:1611.07920 \[hep-ph\]](#).

- [5] R. F. Lebed, R. E. Mitchell, and E. S. Swanson, Heavy-quark QCD exotica, *Prog. Part. Nucl. Phys.* **93**, 143 (2017), [arXiv:1610.04528 \[hep-ph\]](#).
- [6] A. Ali, J. S. Lange, and S. Stone, Exotics: Heavy pentaquarks and tetraquarks, *Prog. Part. Nucl. Phys.* **97**, 123 (2017), [arXiv:1706.00610 \[hep-ph\]](#).
- [7] S. L. Olsen, T. Skwarnicki, and D. Zieminska, Nonstandard heavy mesons and baryons: Experimental evidence, *Rev. Mod. Phys.* **90**, 015003 (2018), [arXiv:1708.04012 \[hep-ph\]](#).
- [8] F.-K. Guo, C. Hanhart, U.-G. Meißner, Q. Wang, Q. Zhao, and B.-S. Zou, Hadronic molecules, *Rev. Mod. Phys.* **90**, 015004 (2018), [Erratum: *Rev. Mod. Phys.* 94, 029901 (2022)], [arXiv:1705.00141 \[hep-ph\]](#).
- [9] R. M. Albuquerque, J. M. Dias, K. P. Khemchandani, A. Martínez Torres, F. S. Navarra, M. Nielsen, and C. M. Zanetti, QCD sum rules approach to the X , Y and Z states, *J. Phys. G* **46**, 093002 (2019), [arXiv:1812.08207 \[hep-ph\]](#).
- [10] Y.-R. Liu, H.-X. Chen, W. Chen, X. Liu, and S.-L. Zhu, Pentaquark and tetraquark states, *Prog. Part. Nucl. Phys.* **107**, 237 (2019), [arXiv:1903.11976 \[hep-ph\]](#).
- [11] F.-K. Guo, X.-H. Liu, and S. Sakai, Threshold cusps and triangle singularities in hadronic reactions, *Prog. Part. Nucl. Phys.* **112**, 103757 (2020), [arXiv:1912.07030 \[hep-ph\]](#).
- [12] N. Brambilla, S. Eidelman, C. Hanhart, A. Nefediev, C.-P. Shen, C. E. Thomas, A. Vairo, and C.-Z. Yuan, The XYZ states: Experimental and theoretical status and perspectives, *Phys. Rep.* **873**, 1 (2020), [arXiv:1907.07583 \[hep-ex\]](#).
- [13] H.-X. Chen, W. Chen, X. Liu, Y.-R. Liu, and S.-L. Zhu, An updated review of the new hadron states, *Rept. Prog. Phys.* **86**, 026201 (2023), [arXiv:2204.02649 \[hep-ph\]](#).
- [14] Y. S. Kalashnikova and A. V. Nefediev, $X(3872)$ in the molecular model, *Phys. Usp.* **62**, 568 (2019), [arXiv:1811.01324 \[hep-ph\]](#).
- [15] S. K. Choi *et al.* (Belle), Observation of a narrow charmonium-like state in exclusive $B^\pm \rightarrow K^\pm \pi^+ \pi^- J/\psi$ decays, *Phys. Rev. Lett.* **91**, 262001 (2003), [arXiv:hep-ex/0309032](#).
- [16] R. Aaij *et al.* (LHCb), Determination of the $X(3872)$ Meson Quantum Numbers, *Phys. Rev. Lett.* **110**, 222001 (2013), [arXiv:1302.6269 \[hep-ex\]](#).
- [17] J. Nieves and M. P. Valderrama, The Heavy Quark Spin Symmetry Partners of the $X(3872)$, *Phys. Rev. D* **86**, 056004 (2012), [arXiv:1204.2790 \[hep-ph\]](#).
- [18] N. A. Törnqvist, From the deuteron to deusons, an analysis of deuteron-like meson meson bound states, *Z. Phys. C* **61**, 525 (1994), [arXiv:hep-ph/9310247](#).
- [19] R. Molina and E. Oset, The $Y(3940)$, $Z(3930)$ and the $X(4160)$ as dynamically generated resonances from the vector-vector interaction, *Phys. Rev. D* **80**, 114013 (2009), [arXiv:0907.3043 \[hep-ph\]](#).
- [20] C. Hidalgo-Duque, J. Nieves, and M. P. Valderrama, Light flavor and heavy quark spin symmetry in heavy meson molecules, *Phys. Rev. D* **87**, 076006 (2013), [arXiv:1210.5431 \[hep-ph\]](#).
- [21] Z.-F. Sun, Z.-G. Luo, J. He, X. Liu, and S.-L. Zhu, A note on the $B^* \bar{B}$, $B^* \bar{B}^*$, $D^* \bar{D}$, $D^* \bar{D}^*$ molecular states, *Chin. Phys. C* **36**, 194 (2012).

- [22] C. Hidalgo-Duque, J. Nieves, A. Ozpineci, and V. Zamiralov, $X(3872)$ and its Partners in the Heavy Quark Limit of QCD, *Phys. Lett. B* **727**, 432 (2013), [arXiv:1305.4487 \[hep-ph\]](#).
- [23] F.-K. Guo, C. Hidalgo-Duque, J. Nieves, and M. P. Valderrama, Consequences of Heavy Quark Symmetries for Hadronic Molecules, *Phys. Rev. D* **88**, 054007 (2013), [arXiv:1303.6608 \[hep-ph\]](#).
- [24] M. Albaladejo, C. Hidalgo-Duque, J. Nieves, and E. Oset, Hidden charm molecules in finite volume, *Phys. Rev. D* **88**, 014510 (2013), [arXiv:1304.1439 \[hep-lat\]](#).
- [25] W. H. Liang, R. Molina, and E. Oset, Radiative open charm decay of the $Y(3940)$, $Z(3930)$, $X(4160)$ resonances, *Eur. Phys. J. A* **44**, 479 (2010), [arXiv:0912.4359 \[hep-ph\]](#).
- [26] E. S. Swanson, $D\bar{D}^*$ and $D^*\bar{D}^*$ molecules, *J. Phys. Conf. Ser.* **9**, 79 (2005).
- [27] M. Albaladejo, F. K. Guo, C. Hidalgo-Duque, J. Nieves, and M. P. Valderrama, Decay widths of the spin-2 partners of the $X(3872)$, *Eur. Phys. J. C* **75**, 547 (2015), [arXiv:1504.00861 \[hep-ph\]](#).
- [28] V. Baru, E. Epelbaum, A. A. Filin, C. Hanhart, U.-G. Meißner, and A. V. Nefediev, Heavy-quark spin symmetry partners of the $X(3872)$ revisited, *Phys. Lett. B* **763**, 20 (2016), [arXiv:1605.09649 \[hep-ph\]](#).
- [29] E. Cincioglu, J. Nieves, A. Ozpineci, and A. U. Yilmazer, Quarkonium Contribution to Meson Molecules, *Eur. Phys. J. C* **76**, 576 (2016), [arXiv:1606.03239 \[hep-ph\]](#).
- [30] V. Baru, C. Hanhart, and A. V. Nefediev, Can $X(3915)$ be the tensor partner of the $X(3872)$?, *JHEP* **06**, 010, [arXiv:1703.01230 \[hep-ph\]](#).
- [31] P. G. Ortega, J. Segovia, D. R. Entem, and F. Fernández, Charmonium resonances in the 3.9 GeV/ c^2 energy region and the $X(3915)/X(3930)$ puzzle, *Phys. Lett. B* **778**, 1 (2018), [arXiv:1706.02639 \[hep-ph\]](#).
- [32] Z.-G. Wang, Analysis of the Hidden-charm Tetraquark molecule mass spectrum with the QCD sum rules, *Int. J. Mod. Phys. A* **36**, 2150107 (2021), [arXiv:2012.11869 \[hep-ph\]](#).
- [33] X.-K. Dong, F.-K. Guo, and B.-S. Zou, A survey of heavy-antiheavy hadronic molecules, *Progr. Phys.* **41**, 65 (2021), [arXiv:2101.01021 \[hep-ph\]](#).
- [34] G. Montaña, A. Ramos, L. Tolos, and J. M. Torres-Rincon, The $X(3872)$, the $X(4014)$, and their bottom partners at finite temperature, (2022), [arXiv:2211.01896 \[hep-ph\]](#).
- [35] X. L. Wang *et al.* (Belle), Study of $\gamma\gamma\rightarrow\gamma\psi(2S)$ at Belle, *Phys. Rev. D* **105**, 112011 (2022), [arXiv:2105.06605 \[hep-ex\]](#).
- [36] M.-Y. Duan, D.-Y. Chen, and E. Wang, The possibility of $X(4014)$ as a $D^*\bar{D}^*$ molecular state, *Eur. Phys. J. C* **82**, 968 (2022), [arXiv:2207.03930 \[hep-ph\]](#).
- [37] Z.-L. Yue, M.-Y. Duan, C.-H. Liu, D.-Y. Chen, and Y.-B. Dong, Hidden charm decays of $X(4014)$ in a $D^*\bar{D}^*$ molecule scenario, *Phys. Rev. D* **106**, 054008 (2022), [arXiv:2208.12796 \[hep-ph\]](#).
- [38] L. Maiani, F. Piccinini, A. D. Polosa, and V. Riquer, The $Z(4430)$ and a New Paradigm for Spin Interactions in Tetraquarks, *Phys. Rev. D* **89**, 114010 (2014), [arXiv:1405.1551 \[hep-ph\]](#).
- [39] J. Wu, X. Liu, Y.-R. Liu, and S.-L. Zhu, Systematic studies of charmonium-, bottomonium-, and B_c -like tetraquark states, *Phys. Rev. D* **99**, 014037 (2019), [arXiv:1810.06886 \[hep-ph\]](#).
- [40] P.-P. Shi, F. Huang, and W.-L. Wang, Hidden charm tetraquark states in a diquark model, *Phys. Rev. D* **103**, 094038 (2021), [arXiv:2105.02397 \[hep-ph\]](#).

- [41] J. F. Giron, R. F. Lebed, and S. R. Martinez, Spectrum of hidden-charm, open-strange exotics in the dynamical diquark model, *Phys. Rev. D* **104**, 054001 (2021), [arXiv:2106.05883 \[hep-ph\]](#).
- [42] B.-Q. Li, C. Meng, and K.-T. Chao, Coupled-Channel and Screening Effects in Charmonium Spectrum, *Phys. Rev. D* **80**, 014012 (2009), [arXiv:0904.4068 \[hep-ph\]](#).
- [43] R. L. Workman *et al.* (Particle Data Group), Review of Particle Physics, *PTEP* **2022**, 083C01 (2022).
- [44] T. Barnes and S. Godfrey, Charmonium options for the $X(3872)$, *Phys. Rev. D* **69**, 054008 (2004), [arXiv:hep-ph/0311162](#).
- [45] T. Barnes, S. Godfrey, and E. S. Swanson, Higher charmonia, *Phys. Rev. D* **72**, 054026 (2005), [arXiv:hep-ph/0505002](#).
- [46] F.-K. Guo, C. Hanhart, Y. S. Kalashnikova, U.-G. Meißner, and A. V. Nefediev, What can radiative decays of the $X(3872)$ teach us about its nature?, *Phys. Lett. B* **742**, 394 (2015), [arXiv:1410.6712 \[hep-ph\]](#).
- [47] M. Ablikim *et al.* (BESIII), Study of Open-Charm Decays and Radiative Transitions of the $X(3872)$, *Phys. Rev. Lett.* **124**, 242001 (2020), [arXiv:2001.01156 \[hep-ex\]](#).
- [48] F.-K. Guo, C. Hanhart, and U.-G. Meißner, On the extraction of the light quark mass ratio from the decays $\psi' \rightarrow J/\psi\pi^0(\eta)$, *Phys. Rev. Lett.* **103**, 082003 (2009), [Erratum: *Phys.Rev.Lett.* 104, 109901 (2010)], [arXiv:0907.0521 \[hep-ph\]](#).
- [49] F.-K. Guo, C. Hanhart, G. Li, U.-G. Meißner, and Q. Zhao, Effect of charmed meson loops on charmonium transitions, *Phys. Rev. D* **83**, 034013 (2011), [arXiv:1008.3632 \[hep-ph\]](#).
- [50] F.-K. Guo, C. Hanhart, and U.-G. Meißner, Extracting the light quark mass ratio m_u/m_d from bottomonia transitions, *Phys. Rev. Lett.* **105**, 162001 (2010), [arXiv:1007.4682 \[hep-ph\]](#).
- [51] E. E. Jenkins, M. E. Luke, A. V. Manohar, and M. J. Savage, Semileptonic B_c decay and heavy quark spin symmetry, *Nucl. Phys. B* **390**, 463 (1993), [arXiv:hep-ph/9204238](#).
- [52] P. Colangelo, F. De Fazio, and T. N. Pham, Nonfactorizable contributions in B decays to charmonium: The Case of $B^- \rightarrow K^- h_c$, *Phys. Rev. D* **69**, 054023 (2004), [arXiv:hep-ph/0310084](#).
- [53] J. F. Amundson, C. G. Boyd, E. E. Jenkins, M. E. Luke, A. V. Manohar, J. L. Rosner, M. J. Savage, and M. B. Wise, Radiative D^* decay using heavy quark and chiral symmetry, *Phys. Lett. B* **296**, 415 (1992), [arXiv:hep-ph/9209241](#).
- [54] J. Hu and T. Mehen, Chiral Lagrangian with heavy quark-diquark symmetry, *Phys. Rev. D* **73**, 054003 (2006), [arXiv:hep-ph/0511321](#).
- [55] S. U. Chung, Spin formalisms, CERN-71-08 [10.5170/CERN-1971-008](#) (1971).
- [56] S. Weinberg, Evidence That the Deuteron Is Not an Elementary Particle, *Phys. Rev.* **137**, B672 (1965).
- [57] V. Baru, J. Haidenbauer, C. Hanhart, Y. Kalashnikova, and A. E. Kudryavtsev, Evidence that the $a_0(980)$ and $f_0(980)$ are not elementary particles, *Phys. Lett. B* **586**, 53 (2004), [arXiv:hep-ph/0308129](#).
- [58] V. Baru, X.-K. Dong, M.-L. Du, A. Filin, F.-K. Guo, C. Hanhart, A. Nefediev, J. Nieves, and Q. Wang, Effective range expansion for narrow near-threshold resonances, *Phys. Lett. B* **833**, 137290 (2022), [arXiv:2110.07484 \[hep-ph\]](#).

- [59] F.-K. Guo, C. Hanhart, U.-G. Meißner, Q. Wang, and Q. Zhao, Production of the $X(3872)$ in charmonia radiative decays, *Phys. Lett. B* **725**, 127 (2013), [arXiv:1306.3096 \[hep-ph\]](#).
- [60] V. Shtabovenko, R. Mertig, and F. Orellana, FeynCalc 9.3: New features and improvements, *Comput. Phys. Commun.* **256**, 107478 (2020), [arXiv:2001.04407 \[hep-ph\]](#).
- [61] V. Shtabovenko, FeynHelpers: Connecting FeynCalc to FIRE and Package-X, *Comput. Phys. Commun.* **218**, 48 (2017), [arXiv:1611.06793 \[physics.comp-ph\]](#).
- [62] H. H. Patel, Package-X 2.0: A Mathematica package for the analytic calculation of one-loop integrals, *Comput. Phys. Commun.* **218**, 66 (2017), [arXiv:1612.00009 \[hep-ph\]](#).
- [63] Y. Dong, A. Faessler, T. Gutsche, and V. E. Lyubovitskij, $J/\psi\gamma$ and $\psi(2S)\gamma$ decay modes of the $X(3872)$, *J. Phys. G* **38**, 015001 (2011), [arXiv:0909.0380 \[hep-ph\]](#).
- [64] S. Uehara, TREPS: A Monte-Carlo Event Generator for Two-photon Processes at e^+e^- Colliders using an Equivalent Photon Approximation, (1996), [arXiv:1310.0157 \[hep-ph\]](#).